DFTT 40/98
CTP-TAMU 31/98
July 1998

Higgs production in charged current six fermion processes at future e^+e^- colliders. [1]

Elena Accomando[a], Alessandro Ballestrero[b] and Marco Pizzio[b]

[a] *Phys. Dept. Texas A&M University*
College Station TX 77843, USA

[b] *I.N.F.N., Sezione di Torino and*
Dipartimento di Fisica Teorica, Università di Torino
v. Giuria 1, 10125 Torino, Italy.

Abstract

We study higgs physics at future e^+e^- colliders taking into account the full set of Feynman diagrams for six fermion final states, which are produced for higgs masses near or above the two W's threshold. In particular we examine events where one isolated lepton or two isolated leptons of different flavours signal the presence of two W*'s. For these charged current processes, a detailed analysis of the relevance of irreducible and QCD background shows that appropriate cuts are generally sufficient to deal with it in the case of reconstructed or missing higgs mass distributions. These latter are however affected by a non negligible distortion and shift of the maximum.

PACS: 11.15.-q; 13.10.+q; 14.70.-e; 14.80.Bn.
Keywords: Higgs boson, Standard Model, Helicity Amplitudes, Linear Collider.

[1] Work supported in part by Ministero dell' Università e della Ricerca Scientifica and by National Science Foundation Grant No. PHY-9722090 (TAMU).

e-mail: accomando@chaos.tamu.edu, ballestrero@to.infn.it

1 Introduction

One of the most challenging present physical issues is the search of the higgs particle and the detailed study of its properties. Precision data fits[1] tend to exclude a higgs heavier than about 300 GeV, and favour a lighter mass. The experimental lower limit for a Standard Model higgs is now of the order of 90 GeV. For the Minimal Supersymmetric Standard Model it is about 10 GeV lower, while theoretical arguments put an upper limit at around 130 GeV[2]. If the higgs is not discovered at LEP2 or Tevatron, its mass will most likely turn out to be higher than 130 GeV. In such a case LHC will probably find it, and the future e^+e^- Linear Collider will be an ideal machine to study its properties, being complementary to the LHC in this respect.

In this paper we analyze Standard Model higgs physics at the Linear Collider supposing that its mass is heavier than about 140 GeV, in the so called intermediate mass region. As it is well known, in such a case the higgs mainly decays into two (possibly virtual) W's and the most important production channels are hZ production (up to 500 GeV) and WW fusion, which dominates at higher energies. The final states to be studied correspond therefore to six fermions, four from the $h \to W^*W^* \to 4f$ decay and two either from the Z decay or the ν_e's in the WW fusion.

Six fermion final states receive contributions from a great number of different Feynman diagrams. Only few of them correspond to higgs production and decay. All the others come from resonant processes (like $t\bar{t}$ or WWZ production), partial resonant (as for instance $\nu_e\bar{\nu}_eWW$) or non resonant ones. All these diagrams, whose number is of the order of several hundreds, correspond to the same final state, interfere among themselves and are to be considered for a complete calculation. Thus, only appropriate cuts can enhance the signal contributions and separate them from the irreducible background which comes from all other diagrams. It should be noticed that different resonant contributions might be considered either as signal or as irreducible background depending on the process under study and their interplay can be consistently analyzed only by complete calculations.

Intermediate mass higgs studies at the Linear Collider have been performed mainly in the *production* $\times$ *decay* approximation (see for instance ref.[3]), where radiative corrections to both production and decay are available [4]. The alternative approach of considering all contributions to a more complete final state as $l\bar{l}WW$, $\nu\bar{\nu}WW$ or $b\bar{b}WW$ has been considered a few years ago[5]. Recently three groups[6][8][9] have started computing full tree level cross sections for six fermion final states at the Linear Collider. These computations have been applied to study the phenomenology of $t\bar{t}$[6][8], WWZ[6] and higgs[9][7] production. In ref.[9] a detailed analysis of $e^+e^- \to \mu^+\mu^- l\bar{\nu}_l u\bar{d}$ ($l = e, \tau$) and of all reactions of the type $e^+e^- \to l^+l^-\nu\bar{\nu}q\bar{q}$ ($q \neq b$) has been performed in connection with higgs physics. In ref. [7] some partial results of the present studies have been summarized.

In the following we systematically study and discuss all relevant 6f processes in which one or more isolated leptons of different flavours make it possible to identify a final state corresponding to the production of two W's. The reason of our choice is simple: these

charged current processes constitute about 52% of the total $hZ \to WWZ$ signal and they are the cleanest processes both from the phenomenological and experimental point of view. In fact, just because of their final state, they allow to get rid of almost all background corresponding to processes in which two W's have not been formed (the only relevant exception corresponds to $l\bar{\nu}q\bar{q}'gg$ which we will examine in detail). For this reason, it is natural to start with studying irreducible backgrounds and realistic mass distributions without the additional complications arising for instance from six jets QCD, ZZZ, or four fermion processes. So we will not consider in this paper six quark final states, which represent about one third of $hZ \to WWZ$ signal but are obviously affected by a severe six jet QCD background. We will also not discuss the properties of six fermion final states which can come from three Z's decay, as it happens for $l\bar{l}\nu\bar{\nu}q\bar{q}$, for 4 quarks with a couple $l\bar{l}$ of same flavour leptons, and for 4 q's + 2 ν's. Out of these last three processes the first, which corresponds to about 2.6% of $hZ \to WWZ$ signal and may also be affected by $t\bar{t}$ background, has already been discussed in the literature [9]. The other two represent respectively around 4.4% and 8.8% of $hZ \to WWZ$ signal and their ZZZ and QCD backgrounds have to be carefully analyzed. In the case of 4 q's + 2 ν's and $l\bar{l}\nu\bar{\nu}q\bar{q}$, also four fermion processes can be dangerous and must be considered.

Being interested in higgs signal, one has of course always to deal with WWZ background, but this is really irreducible in the sense that it cannot be eliminated just by choosing a particular set of final states. A careful study of distributions and of possible cuts is therefore unavoidable.

The plan of the paper is the following. In sect. 2 we give some detail of the processes and of the method used for their calculation. In section 3 we examine the results for final states with 2 quarks and in section 4 those with four quarks. We draw some conclusions in section 5.

2 Processes and their calculation

As already mentioned in the introduction, we will consider in detail processes with one isolated lepton like $l\,\nu_l\,+\,4\,q's$ or $l\,\nu_l\,+\,l'\,\bar{l}'\,+\,2\,q's$, and those with missing energy and two leptons of different flavour and charge like $l\,\nu_l\,+\,l'\,\nu_{l'}\,+\,2\,q's$. We use $l\,\nu_l$ to indicate both $l^-\,\bar{\nu}_l$ and $l^+\,\nu_l$. The first two cases represent respectively about 31% and 4.4% of $hZ \to WWZ$ signal, while the third one amounts to about 4.1% ($q \neq b$), as one simply deduces from W and Z branching ratios. Let us notice that for the first two final states, the isolated lepton plus missing energy indicates that most likely two $W's$ have been formed in the process. The same indication is given in the third process by the two isolated leptons of different flavour and charge, which imply the presence of their corresponding neutrinos. We will not explicitly discuss the final state $l\,\nu_l + l'\,\nu_{l'} + l''\,\bar{l}''$, as it amounts only to .7% of the $hZ \to WWZ$ events and it is very similar to $l\,\nu_l\,+\,l'\,\bar{l}'\,+\,2\,q's$.

All calculations have been performed with the program SIXPHACT, which has already been used for $t\bar{t}$ and WWZ studies[6]. In the present version we have added

the diagrams containing higgs exchanges and other mappings for the phase space, in order to account for the resonant peaking structures corresponding to higgs events. A detailed description of how the computation is organized can be found in ref. [6]. At present the program can compute all charged current (CC) 6f final states, i.e. those final states which can derive from the decay of two W's and a Z, but cannot reconstruct the ones coming from three Z's. All tree level Feynman diagrams are exactly evaluated in an helicity amplitude formalism[10]. Their number is at least of the order of 200 when no exchanges among identical particles are possible. If we consider for instance final states with one isolated lepton and four quarks, $\mu\bar{\nu}u\bar{d}b\bar{b}$ has 232 diagrams (23 of which are due to higgs) and $e\bar{\nu}u\bar{d}u\bar{u}$ 840 (4 with higgs).

SIXPHACT can account for initial state radiation (ISR), beamstrahlung (BMS) with a link to CIRCE[11], naive QCD corrections (exact in *production* $\times$ *decay* no cuts limit). It has exact b and t fermion masses both in the amplitudes and in the phase space. All results given in the following have been computed with ISR, BMS, NQCD. CPU times depend of course on the particular final processes, on the cuts, and the options required. As an indication, a process like $e^+e^- \to \mu^+\mu^- e\bar{\nu}_e u\bar{d}$ (418 diagrams) with ISR, BMS and NQCD takes about 20 minutes for 3 per mille, 3 hours for per mille and one day for .2 per mille accuracy on a DEC ALPHA station.

For the numerical part we have used $s^2_{_W} = 1 - M^2_{_W}/M^2_{_Z}$, $\quad g^2 = 4\sqrt{2}G_\mu M^2_{_W}$ and the input masses $m_Z = 91.1888$ GeV, $m_W = 80.23$ GeV. We have chosen $m_t = 175$ GeV and for m_b the running mass value $m_b = 2.7$ GeV. For the strong corrections to Z, W, t and h decay widths and vertices we have used $\alpha_s(m_Z) = 0.123$ and let it evolve to the appropriate scales.

We have implemented the following general set of cuts, appropriate for the Linear Collider studies:

jet(quark) energy > 3 GeV; $\quad$ lepton energy > 1 GeV; $\quad$ jet-jet mass > 10 GeV;
lepton-beam angle $> 10°$; $\quad$ jet-beam angle $> 5°$; $\quad$ lepton-jet angle $> 5°$.

For the different processes we have sometimes used other cuts which will be described in due time.

In the following we will mainly study invariant mass distributions, from which one can hope to extract informations on higgs mass and width and study appropriate cuts. An example of these distributions is given in fig. 1 for the process $\mu\bar{\nu}u\bar{d}b\bar{b}$. Here and in the following figures, we do not report the errors on the single bins as the statistical precision is such that they are practically not distinguishable on the plots. The distributions in fig. 1 are obtained with signal diagrams only. In practice, apart from the off-shellness of higgs, W's and Z and from spin correlations, these distributions correspond to the ones one would obtain in the *production* $\times$ *decay* approximation. In the upper part of the figure we have used a logarithmic scale. The three curves correspond to the exact higgs (i.e. $\mu\bar{\nu}u\bar{d}$) distribution (continuous line), to the reconstructed mass (dashed) and to the missing one (chaindot). As it is obvious, the exact $\mu\bar{\nu}u\bar{d}$ invariant mass distribution cannot be experimentally determined, due to the fact that the neutrino four momentum cannot be measured. One can try to reconstruct it

from the missing momentum and energy. But the presence of ISR and BMS, which also contribute to the missing momentum and energy, introduces an error in this determination. The best one can do is to ascribe all missing 3-momentum to the neutrino and determine its energy from the on shell condition. We name reconstructed mass the one obtained by using this approximately reconstructed 4-momentum. The missing distribution corresponds instead to the invariant mass of the 4-momentum recoiling against the particles (b's in this case) decaying from the Z. In absence of ISR and BMS this would be the exact $\mu\bar{\nu}u\bar{d}$ invariant mass. Fig. 1 shows clearly the differences between the two approximated, more realistic, distributions and the exact one. In particular, in the lower part of the figure the difference between reconstructed and missing mass is reported in a linear scale. Of the two, the latter is much more distorted. This feature is not peculiar of the specific final state considered. It is therefore evident that, whenever possible, the reconstructed mass will be measured and studied.

3 Final states with two quarks.

In this section we will examine processes of the type $l\,\nu_l + l'\,\bar{l}' + 2\,q's$ and $l\,\nu_l + l'\,\nu_{l'} + 2\,q's$ ($q \neq b$). Even if the two final states together only amount to about 10% of the $hZ \to WWZ$ signal, they are a priori particularly interesting as they have neither QCD nor $t\bar{t}$ background. With q we denote here any light quark u, d, c, s, so one can actually measure the second reaction only if one excludes the b's with b-tagging. Otherwise one has to face the huge $t\bar{t}$ background.

For the first type reaction we consider $e\bar{\nu}u\bar{d}\mu^+\mu^-$. At 500 GeV the signal cross section for $m_h = 200$ GeV is 0.03501(2) fb, while the total one is 0.07824(3) fb. As usual we indicate in brackets the error on the last digit and we have applied two additional cuts: $|m(\mu^+\mu^-) - m_Z| < 20$ GeV and $|m(u\bar{d}) - m_W| < 20$ GeV. The two cross sections above show that the irreducible background given by all non higgs diagrams can often be of the same order or even bigger than the signal. In practice however one does not have to worry about this fact. This is evident from fig. 2, where the reconstructed mass distribution is reported for the total cross sections (for $m_h = 150, 170, 200, 250$ GeV) and the background only (continuous line). One can see that the part of the background under the higgs mass peaks is almost irrelevant. In fact, considering an interval of 20 GeV around the peak, the ratio SB between signal and background for m_h =200 GeV is 10.0 at 500 GeV and 14.0 at 360 GeV. In the worst case reported in the figure, namely at m_h =250 GeV, SB is 5.1 at 500 GeV and 3.7 at 360 GeV. As it is obvious the background in this case receives its greatest contribution from WWZ resonant diagrams. The fact that it is not important when considering invariant mass distributions is of course common to all processes and not specific to the one at hand. Another general feature that can be easily seen in fig. 2 is that the signal for m_h =150 GeV, which is below WW threshold, is clearly visible. This happens even if we have applied a cut on $m(u\bar{d})$ in order to constrain it to be in the vicinity of the W mass.

It is interesting to evaluate also the signal to square root of background ratio SSB. We do this always by considering an interval of 20 GeV around the nominal higgs mass,

by assuming a luminosity of $50 fb^{-1}$ and multiplying both signal and background by 8 to approximately account for the multiplicity of the analogous channels. For $l\nu_l + l'\bar{l}' + 2q's$ and $l\,\nu_l\, +\, l'\,\nu_{l'}\, +\, 2\,q's\,(q \neq b)$, a factor ≈ 4 accounts for the different q's and a factor ≈ 2 for choosing $l = e$ and $l' = \mu$ or viceversa. Of course the SSB numbers improve by more than a factor 3 for the higher luminosity option of $500 fb^{-1}$, and this might be important for high higgs masses. For m_h =200 GeV SSB is 10 at 500 GeV and 15 at 360 GeV; at m_h =250 GeV, SSB is 5.7 at 500 GeV and 4.1 at 360 GeV.

As far as $l\,\nu_l\, +\, l'\,\nu_{l'}\, +\, 2\,q's$ is concerned, let us consider specifically $\mu\bar{\nu}e^+\nu s\bar{s}$. For this reaction we apply only the additional cut $|m(s\bar{s}) - m_Z| < 20$. Also in this case if we consider the total cross section and the signal one we find that the background can be of the same order of the signal. For instance at 500 GeV for $m_h = 170$ GeV the total cross section is 0.14498(3) fb and the signal amounts to 0.08077(1) fb. So we must consider the invariant mass distributions. In this case the reconstructed mass is not experimentally viable, so one looks at the missing one. The distributions are reported in fig. 3. Once again one can compute SB and SSB for m_h =200 and 250 GeV. At lower m_h the background is less and less relevant. In the first case we have SB=7.9, SSB=8.5 at 500 GeV and SB=13.5, SSB=16.5 at 360 GeV. In the latter, one finds respectively SB=3.6, SSB=4.8 and SB=3.1, SSB=4.5. It has however to be noticed that the signal missing mass distributions are very asymmetric and their form is rather unrealistic. We have therefore examined the case in which the mass reconstruction is affected by a gaussian "experimental error" of 5 GeV. This means that every missing mass computed by our program has been displaced with a gaussian probability whose standard deviation is 5 GeV. With this we try to simulate in a very simple and qualitative way the uncertainties introduced by the hadronization and the reconstruction from real particles of the invariant mass. The result is reported in fig. 4. One may notice that the smearing makes the distributions more symmetric, but it produces a sizeable shift of the maximum of the order of a few GeV. This is a feature that has to be carefully taken into account when one wants to study higgs properties in processes with two neutrinos or in general using missing mass distributions. As a consequence of these results and since the branching ratio of this channel is not more than 5%, our conclusion is that $l\,\nu_l\, +\, l'\,\nu_{l'}\, +\, 2\,q's$ is not a very good candidate for higgs studies. Including all possible final states with two ν's and 2 or 4 leptons, the total branching ratio increases up to about 8.8%, but in that case the huge background from ZZ into four fermions could also affect the final state with two charged leptons of the same flavour.

4 Final states with four quarks and one isolated lepton.

Final states with four quarks and one isolated lepton correspond to about one third of higgs $hZ \to WWZ$ events. They are however affected by $t\bar{t}$ and QCD background. The latter may come from both 2 gluons + 2 quarks + $l\nu$ events and from the contribution

to the usual $l\nu + 4q's$ final state due to diagrams with gluon exchange between the two quark lines.

One may consider processes with or without 2 b's in the final state. They can be distinguished with b-tagging, although one has to take into account that such an identification has always some degree of error. If two b's and one isolated lepton are present, the event cannot correspond to 2 gluons + 2 quarks + $l\nu$ production, and one does not have to worry about such background. Moreover if a Z has been produced, the two b's are necessarily its decay products. So one can apply a cut, forcing the $b\bar{b}$ invariant mass to be in the vicinity of M_Z. This kind of cut does not reduce the higgs signal, while it strongly suppresses QCD background coming from gluon exchange diagrams. With two b's in the final states, the largest background is that due to $t\bar{t}$ production and decay. The above mentioned cut is efficient also in this case, as one does not expect that the b's coming from $t\bar{t}$ decay prefer an invariant mass near the Z. However the $t\bar{t}$ cross section is about 10 times bigger than the $hZ \to W^+W^-b\bar{b}$ production. Therefore one has to carefully compute the effects of the $b\bar{b}$ cut. In the upper part of fig. 5 we present the contribution of the background to the distributions of the true, reconstructed and missing invariant higgs mass for $\mu\bar{\nu}u\bar{d}b\bar{b}$, computed by imposing that $|m(u\bar{d}) - m_W|$ <20 GeV and $|m(b\bar{b}) - m_Z|$ <20 GeV. Only the latter cut is relevant to the $t\bar{t}$ production cross section which is reduced by a factor 5.

If one takes the other possibility and excludes $b\bar{b}$ events, one does not have to worry about $t\bar{t}$ (apart from imperfect b-tagging), but QCD and EW backgrounds have to be considered. As far as the signal is concerned, there are no important differences with respect to the $b\bar{b}$ case, apart for the fact that one can now sum over the different light flavours emitted by the Z. We do not report the plot equivalent to fig. 1 for the signal with $s\bar{s}$ instead of $b\bar{b}$, just because the differences are at percent level even if the cuts are now different. In fact having 4 light quarks in the final state, it is not known which jets are produced by the Z decay and which by the W. Therefore we choose to accept the event if at least one pair of couples qq', $q''q'''$ is such that $|m(qq') - m_Z|$ and $|m(q''q''') - m_W|$ are less than 20 GeV. This cut is applied also in the following to all results with four light quarks in the final state.

In the lower part of fig. 5 one can see the background for $\mu\bar{\nu}u\bar{d}s\bar{s}$, due to EW diagrams and to diagrams with gluon exchange. The curves marked QCD refer only to this irreducible background and not to $qq + gg + l\nu$. The process $\mu\bar{\nu}u\bar{d}s\bar{s}$ is obviously not experimentally distinguishable, but it has been considered here because it is at all similar to $\mu\bar{\nu}u\bar{d}b\bar{b}$ without single and double resonant top diagram contributions. The tiny differences due to b mass are not relevant in this context. By comparing the upper and the lower part of fig. 5, one therefore concludes that the irreducible background coming from $t\bar{t}$ production and decay is more important by a factor of order 30 than the remaining EW contributions. The irreducible background coming from gluon exchange is completely irrelevant as it is about three order of magnitudes less than the $t\bar{t}$ one.

In fig. 6 we study the importance of the various backgrounds when there is no $b\bar{b}$ pair in the final state. In order to consider a realistic cross section we sum over all remaining $q\bar{q}$ flavours ($q = u, d, c, s$). The upper part of fig. 6 leads to the same conclusions as the

lower one of fig. 5 for the irreducible background via gluon exchange: the curve marked $QCD \times 20$, which corresponds to this background multiplied by a factor 20 is still lower than the EW one, thus confirming its complete irrelevance. In the lower part of fig. 6 we report the background coming from $\mu\bar{\nu}u\bar{d}gg$ final state. This turns out to be almost as important as the EW one. We remind that in this case the EW does not contain any contribution from $t\bar{t}$ states. In the following we will not sum the $l\bar{\nu}q\bar{q}'gg$ background to the irreducible EW one, because it is conceivable that it may be further reduced by experimental cuts or by the possibility to distinguish among quark and gluon jets. Moreover, it is immediate to evaluate it from fig. 6 and we will see in the following that the irreducible background not coming from $t\bar{t}$ is of scarce significance even if one multiplies it by an approximate factor two, to account for two quark plus two gluon jets.

Coming to a more specific analysis of signal-background interplay, let us consider the process $\mu\bar{\nu}u\bar{d}b\bar{b}$. Processes of this type with two b's are of the order of 6.5% of total $hZ \to WWZ$ signal. In fig. 7 we show the reconstructed mass distribution for the background and for the complete cross sections corresponding to m_h =150, 170, 200, 250 GeV. One notices immediately in the lower part of the figure that up to 200 GeV the cut $|m(b\bar{b}) - m_Z|$ <20 GeV is certainly sufficient. For $m_h = 200$ GeV the ratio SB is 1.4 and SSB is 8.1, while for $m_h = 250$ GeV one gets SB=.2 and SSB=2.5. In the latter case, the number of signal events is 29.7 while the background events are 139. For the processes in this section the factor 8, by which we have multiplied signal and background, approximately corresponds to the possibility of having isolated electrons or muons of different charge and $c\bar{s}$ in place of $u\bar{d}$. In the upper part of fig. 7 we compute the effects on the distribution of an additional cut regarding the invariant mass of the top. For top events, $u\bar{d}b$ reconstructs the mass of the top. As one cannot distinguish b from $\bar{b}$ experimentally, we impose that $|M - m_{top}|$ >40 GeV both for $M = m(bu\bar{d})$ and for $M = m(\bar{b}u\bar{d})$. From the comparison of the lower and upper part of fig. 7, one deduces that such a cut reduces the signal by about a factor 2.5, but SB and SSB become respectively 6.0 (2.8) and 10.2 (5.2) for $m_h = 200(250)$ GeV, still leaving 9.6 events when $m_h = 250$ GeV.

If one excludes the b's and considers only final states with light quarks, the corresponding distribution is represented in the upper part of fig. 8 where we sum over the quark flavours as indicated in the plot, taking properly into account the additional contributions arising in the case when identical quarks are present in the final state. One can see that the situation is very clean. The background from non perfect b-tagging is not taken into account and depends on the probability that a b is misidentified. One can however have an idea of its importance considering the extreme case in which there is no b-tagging at all, as we do in the following.

It is interesting to examine the case in which one simply sums over all quark flavours (u, d, c, s, b) for the $q\bar{q}$ pairs, since the higgs signal of course increases in this case. The corresponding distribution is presented in the lowest part of fig 8. In this case also for the $b\bar{b}$ events the cuts are the same as for light quarks: $|m(qq') - m_Z|$ <20 GeV and $|m(q''q''') - m_W|$ <20 GeV as explained before. One immediately deduces from

the figure that below $m_h \approx 180$ GeV the signal can be measured without any problem. But also for higher masses the situation is not bad: even if at m_h =200 (250) GeV SB is .7(.4), SSB is 12.2(7.4). It would be possible, if necessary, to impose cuts on the invariant masses of three jets, rejecting events in which any jet triplet form an invariant mass in the vicinity of the top.

Finally in fig. 9 we have examined the possible effects on the distributions of the experimental error in the determination of the reconstructed higgs mass. We have assumed a 5 GeV gaussian error as before. One can see that the shape of the signal distributions changes rather significantly, but as far as SB and SSB is concerned the difference is almost irrelevant: SB=.7(.4) SSB=11.6(6.8) at 200(250) GeV.

5 Conclusions

By means of complete 6f calculations performed with SIXPHACT, we have examined higgs processes with one or two isolated leptons of different flavour in the final state, in order to eliminate as much as possible the background not containing two W's. We have moreover applied cuts to eliminate $t\bar{t}$ and studied reconstructed and missing invariant mass distributions at 500 and 360 GeV.

The main results may be summarized as follows.

For processes $l\,\nu_l + l'\,\bar{l}' + 2\,q's$, where QCD and $t\bar{t}$ background are absent, the signal is very clean and the background has hardly any effect around the reconstructed higgs invariant mass. Even *production* $\times$ *decay* approximation could be used in that region, while for the total cross section the contribution of the irreducible background can be of the same order of the signal.

The same applies to $l\,\nu_l + l'\,\nu_{l'} + 2\,q's\,(q \neq b)$, but in this case one has to consider the missing energy which entails a substantial distortion and a shift of some GeV in the distribution. As b-tagging might moreover leave in practice a part of $t\bar{t}$ background, it seems that this reaction is not the best candidate for higgs studies.

The processes $l\,\nu_l + 4\,q's$ with four quarks correspond to about one third of $hZ \to WWZ$ signal and are therefore more important. Irreducible QCD background due to diagrams with gluon exchange is completely irrelevant. The one coming from $l\bar{\nu}q\bar{q}'gg$ is of the same order of the electroweak one and has little practical effect. The main source of background comes from $t\bar{t}$ production and decay. It turns out that it can be kept under control, at least for not too high higgs masses, both if one sums over all final state quarks or if one looks specifically for a $b\bar{b}$ couple in the final state.

References

[1] The LEP Collaborations ALEPH, DELPHI, L3, OPAL, the LEP Electroweak Working Group and the SLD Heavy Flavour Group. CERN PPE/97-154.

[2] M. Carena, J.R. Espinosa, M. Quiros and C.E.M. Wagner, *Phys. Lett.* 355B (1995) 209 ; H. Haber, R. Hempfling and A.H. Hoang, *Z. Phys.* C57 (1997) 539 ;
S. Heinemeyer, W. Hollik and G. Weiglein, prep. KA-TP-13-1998, hep-ph/9807423.

[3] P. Grosse Wiesmann, D. Haidt and H.J. Schreiber, in: P. M. Zerwas (ed.) "e^+e^- Collisions at 500 GeV: The Physics Potential - Part A" - Desy 02-123A (1992) pg. 37.

[4] A. Djouadi, P. Gambino, B.A. Kniehl, *Nucl. Phys.* 523B (1998) 17;
for a complete review see: B.A. Kniehl *Phys. Rep.* 240 (1994) 211.

[5] V. Barger, K. Cheung, A. Djouadi, B.A. Kniehl, R.J.N. Phillips and P.M. Zerwas, in: P. M. Zerwas (ed.) "e^+e^- Collisions at 500 GeV: The Physics Potential - Part C" - Desy 02-123C (1993) pg. 5;
A. Ballestrero, E. Maina, S. Moretti, *Phys. Lett.* B333 (1994) 434;
A. Ballestrero, E. Maina, S. Moretti, *Phys. Lett.* B335 (1994) 460.

[6] E. Accomando, A. Ballestrero, M. Pizzio, *Nucl. Phys.* B512 (1998) 19.

[7] E. Accomando, A. Ballestrero, M. Pizzio, in: R. Settles (ed.) "e^+e^- Linear Colliders: Physics and Detector Studies, Part E", DESY 97-123E (1997) pg. 31.

[8] F. Yuasa, Y. Kurihara, S. Kawabata, *Phys. Lett.* B414 (1997) 178.

[9] G. Montagna, M. Moretti, O. Nicrosini, F. Piccinini, *Eur. Phys. J.* C2 (1998) 483;
F. Gangemi,G. Montagna, M. Moretti, O. Nicrosini, F. Piccinini, in: R. Settles (ed.) "e^+e^- Linear Colliders: Physics and Detector Studies, Part E", DESY 97-123E (1997) pg. 393, hep-ph/9811437.

[10] A. Ballestrero, E. Maina, *Phys. Lett.* B350 (1995) 225.

[11] T. Ohl, *Comp. Phys. Commun.* 101 (1997) 269.

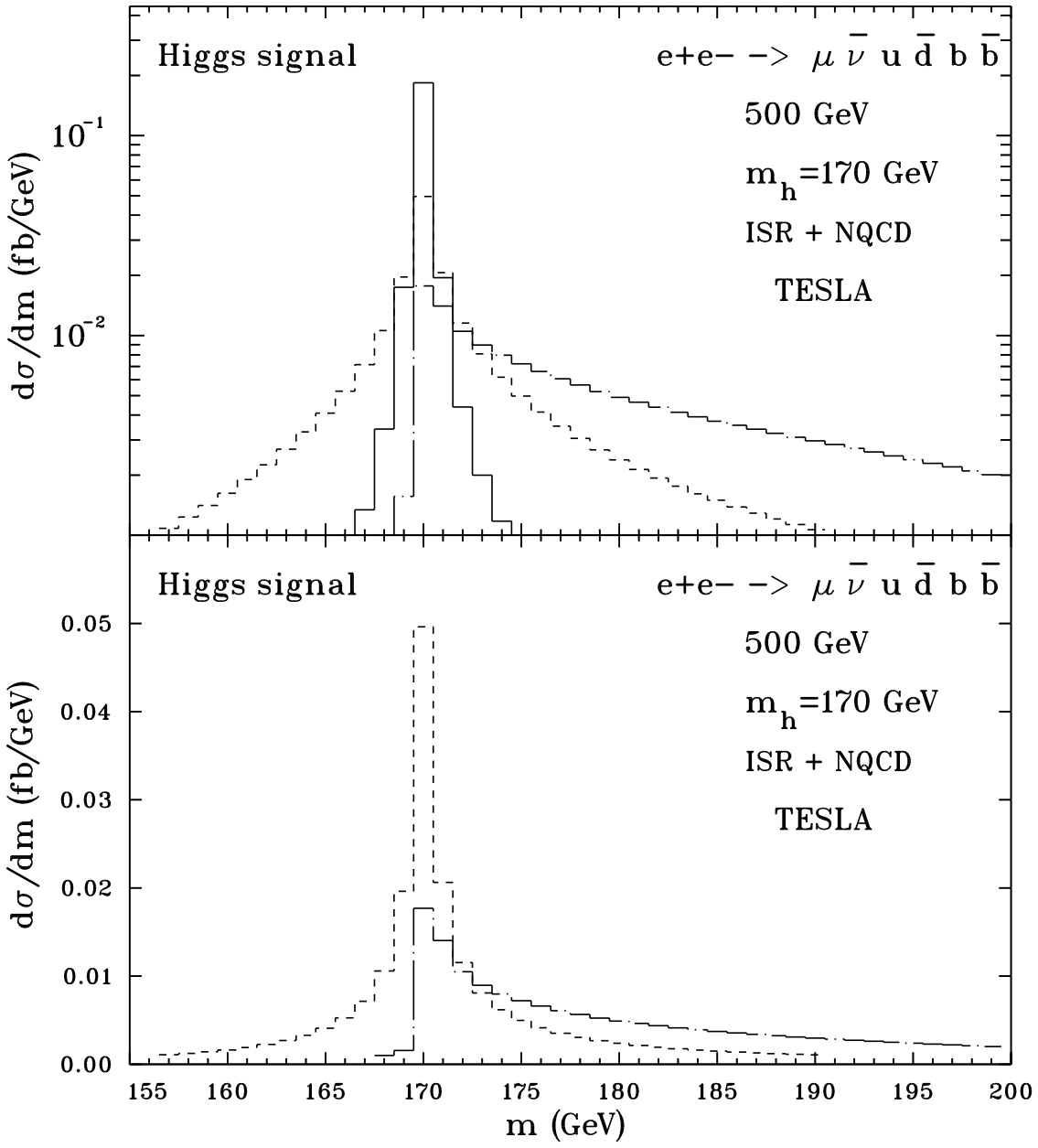

Figure 1: Invariant mass distributions for higgs signal. The continuous line corresponds to $(\mu\bar{\nu}u\bar{d})$ mass, the dashed line to the *reconstructed* and the chaindot to the *missing* one. Cuts: $|m(b\bar{b}) - m_Z| < 20$ GeV, $|m(u\bar{d}) - m_W| < 20$ GeV.

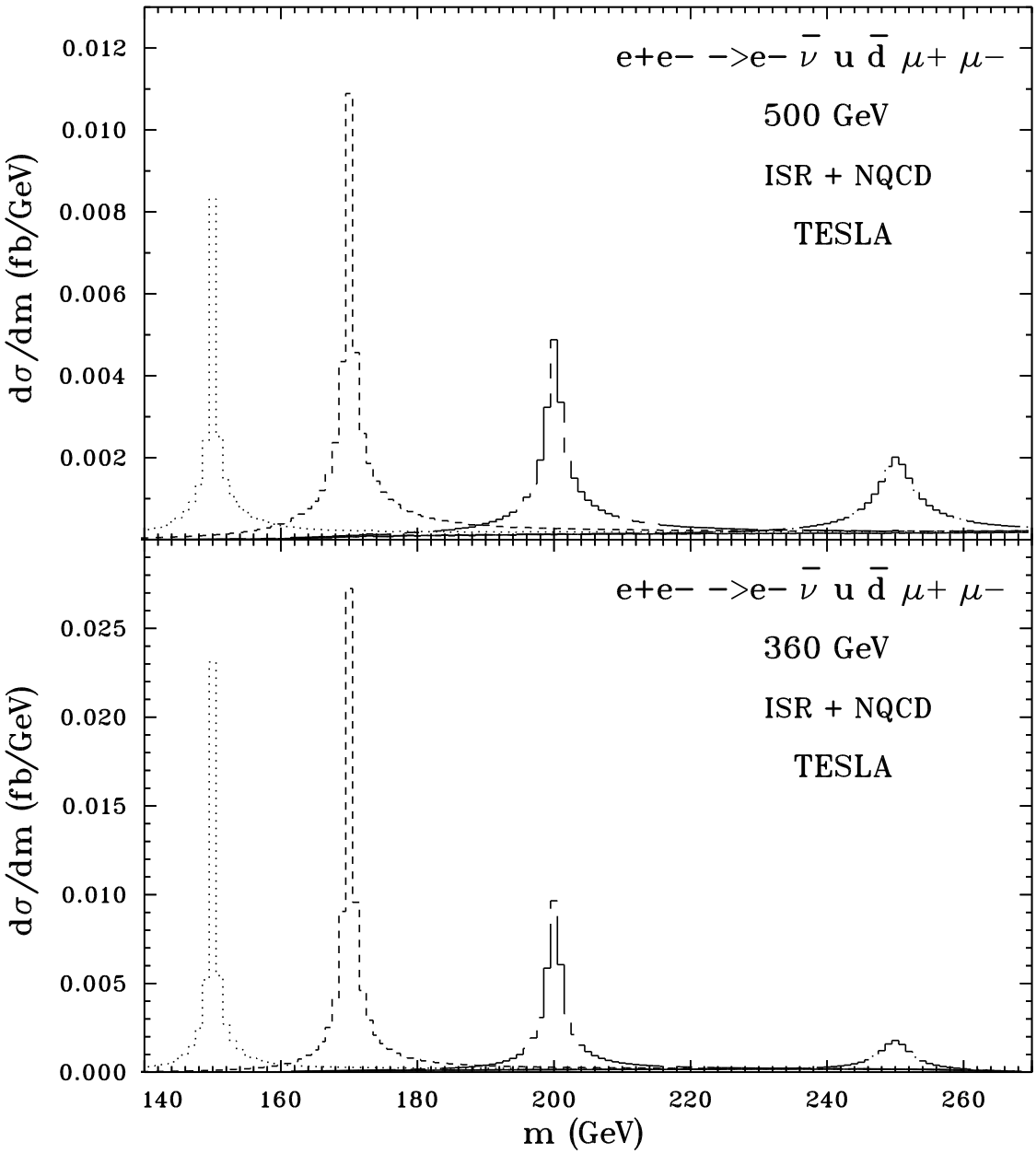

Figure 2: Reconstructed mass distributions The continuous line represents the total background. The others correspond to the total cross sections for (from left to right) m_h= 150, 170, 200, 250 GeV. Cuts: $|m(\mu^+\mu^-) - m_Z| < 20$ GeV, $|m(u\bar{d}) - m_W| < 20$ GeV.

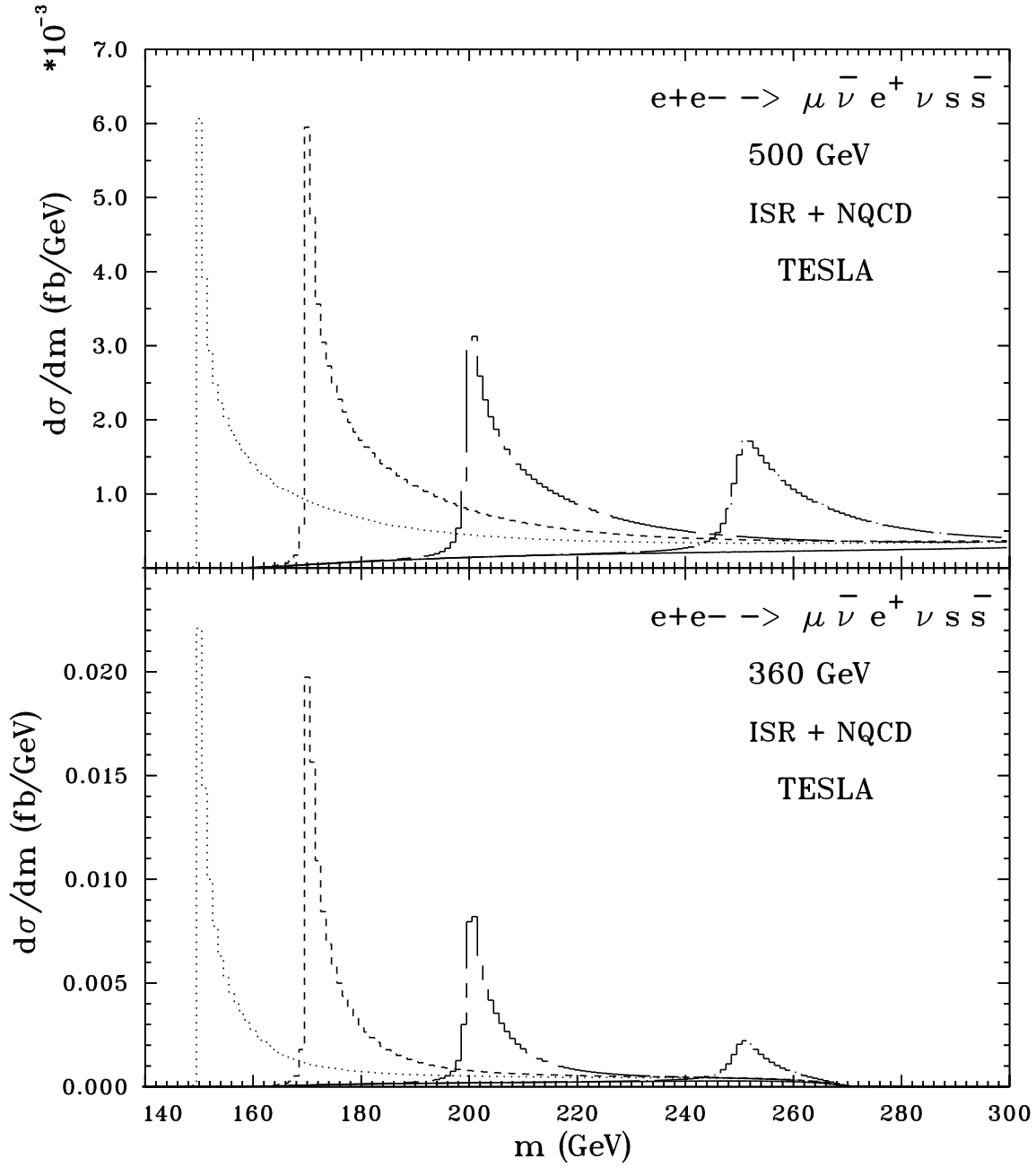

Figure 3: Missing mass distributions. The continuous line represents the total background. The others correspond to the total cross sections for (from left to right) m_h= 150, 170, 200, 250 GeV. Cuts: $|m(s\bar{s}) - m_Z| < 20$ GeV.

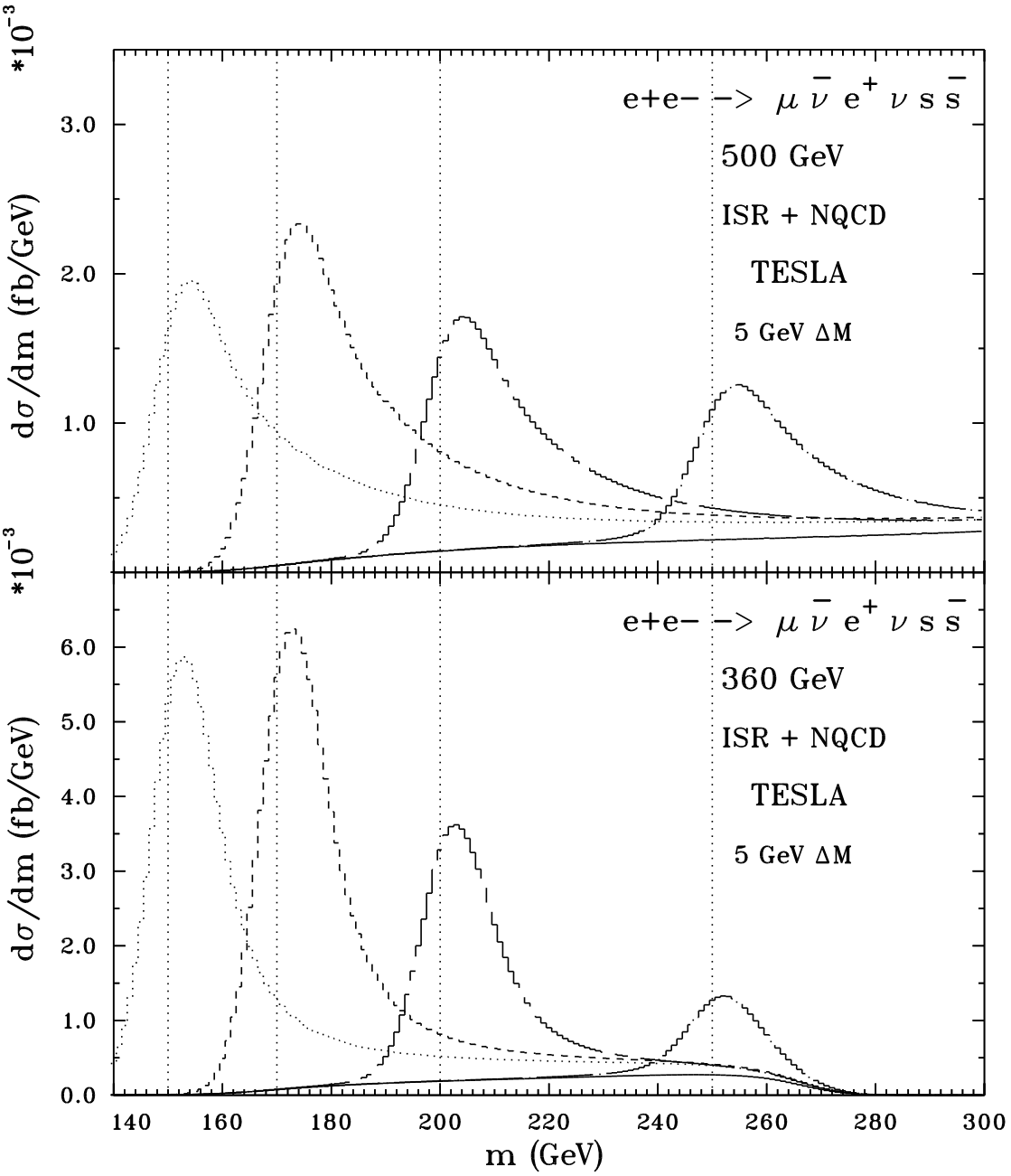

Figure 4: Missing mass distributions with gaussian smearing. The continuous line represents the total background. The others correspond to the total cross sections for (from left to right) m_h= 150, 170, 200, 250 GeV. Cuts: $|m(s\bar{s}) - m_Z| < 20$ GeV.

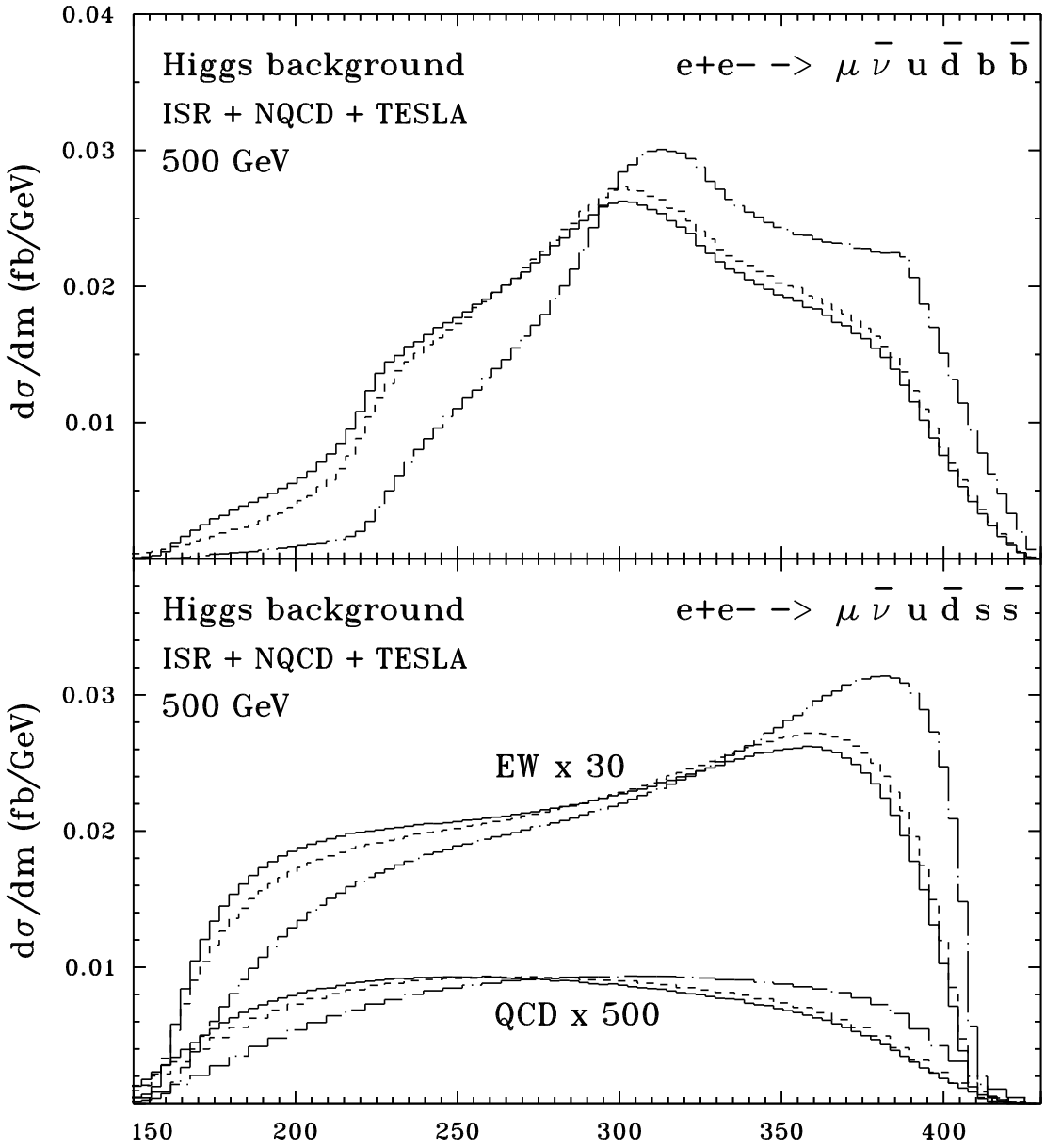

Figure 5: Invariant mass distributions for higgs background. The continuous line corresponds to $(\mu\bar{\nu}u\bar{d})$ mass, the dashed line to the *reconstructed* and the chaindot to the *missing* one. Cuts: $|m(u\bar{d}) - m_W| < 20$ GeV, $|m(q\bar{q}) - m_Z| < 20$ GeV ($q = b$ or s).

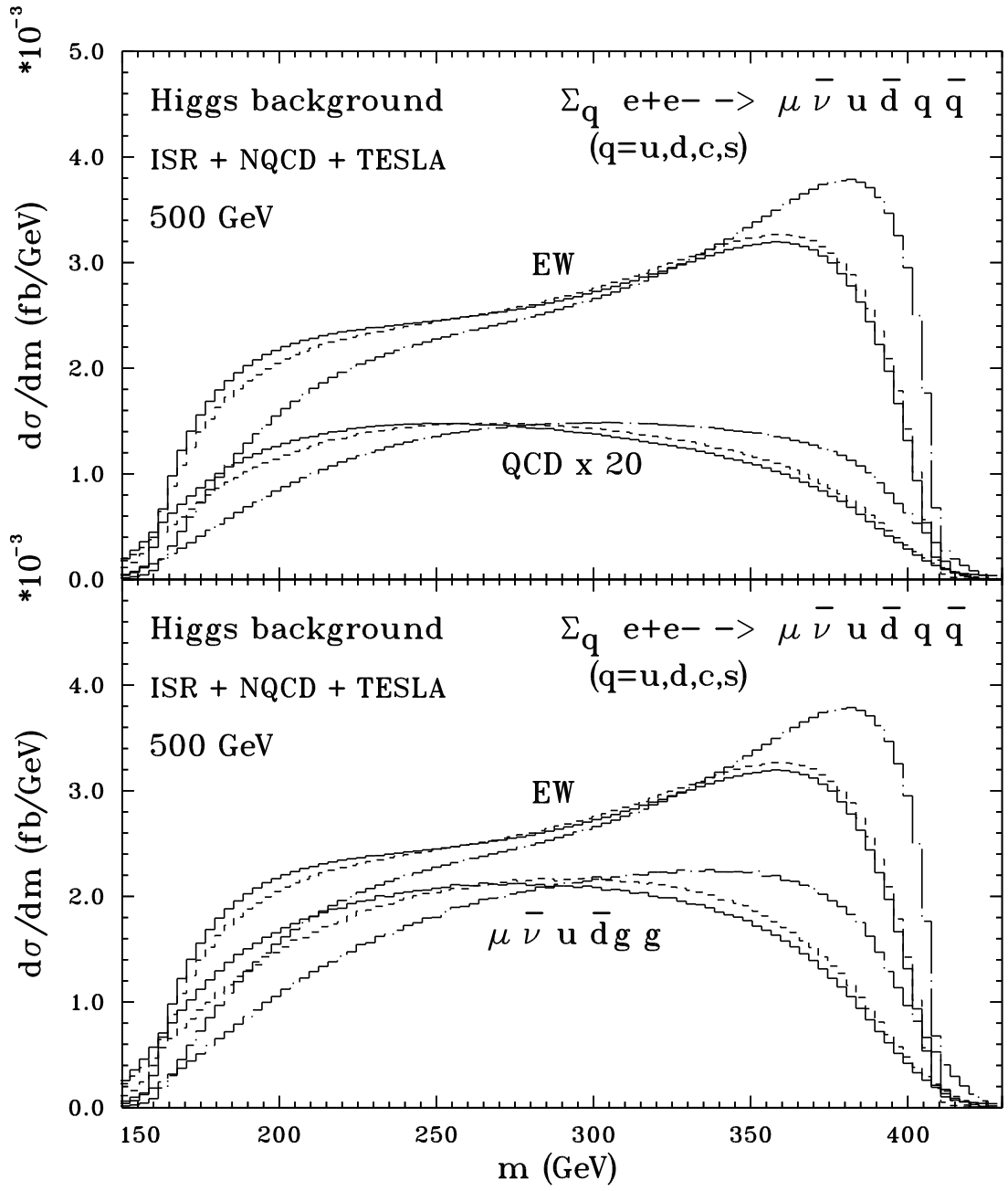

Figure 6: Invariant mass distributions for higgs background. The continuous line corresponds to ($\mu\bar{\nu}u\bar{d}$) mass, the dashed line to the *reconstructed* and the chaindot to the *missing* one. Cuts: $|M_1 - m_Z| < 20$ GeV, $|M_2 - m_W| < 20$ GeV. M_1 and M_2 are the invariant masses of the pairs of strong particles which are contemporarily nearer to m_Z and m_W.

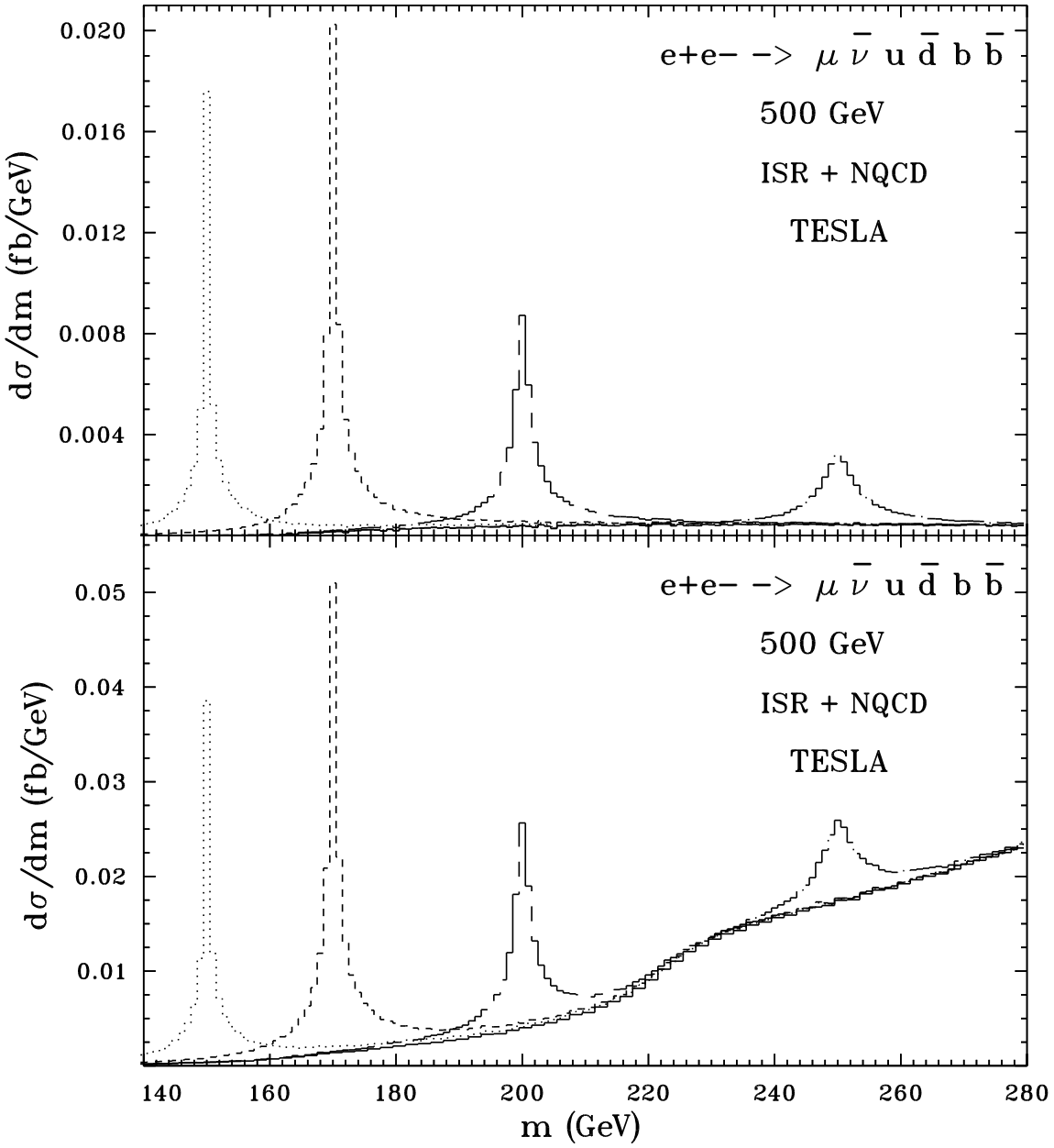

Figure 7: Reconstructed mass distributions with $|m(b\bar{b}) - m_Z|$ and $|m(u\bar{d}) - m_W| < 20$ GeV and, in the upper part only, $|M - m_{top}| > 40$ GeV ($M = m(bu\bar{d})$ and $m(\bar{b}u\bar{d})$). The continuous line represents the total background. The others correspond to the total cross sections for (from left to right) m_h= 150, 170, 200, 250 GeV.

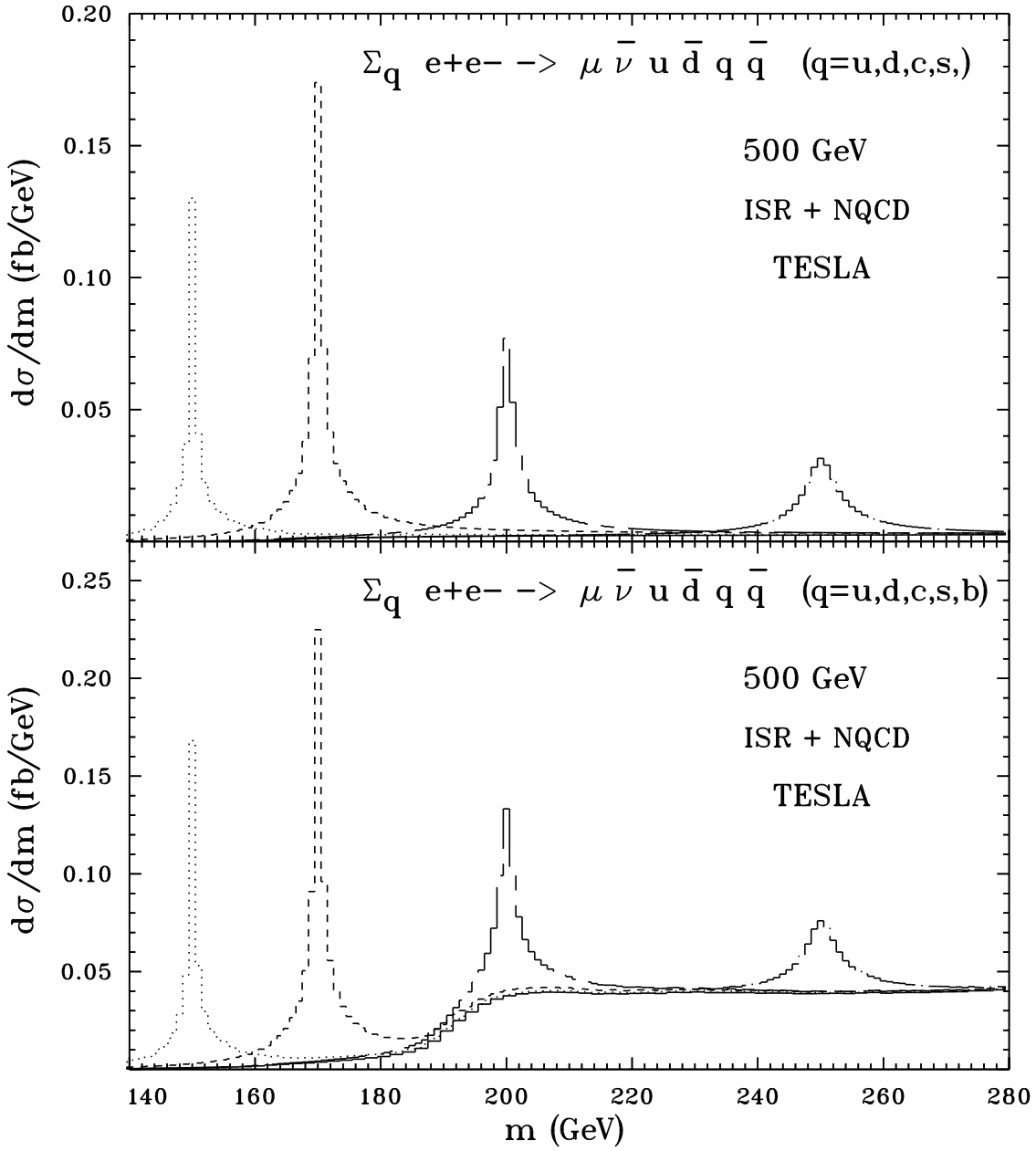

Figure 8: Reconstructed mass distributions. The continuous line represents the total background. The others correspond to the total cross sections for (from left to right) m_h= 150, 170, 200, 250 GeV. Cuts: $|m(q\bar{q}) - m_Z| < 20$ GeV, $|m(u\bar{d}) - m_W| < 20$ GeV.

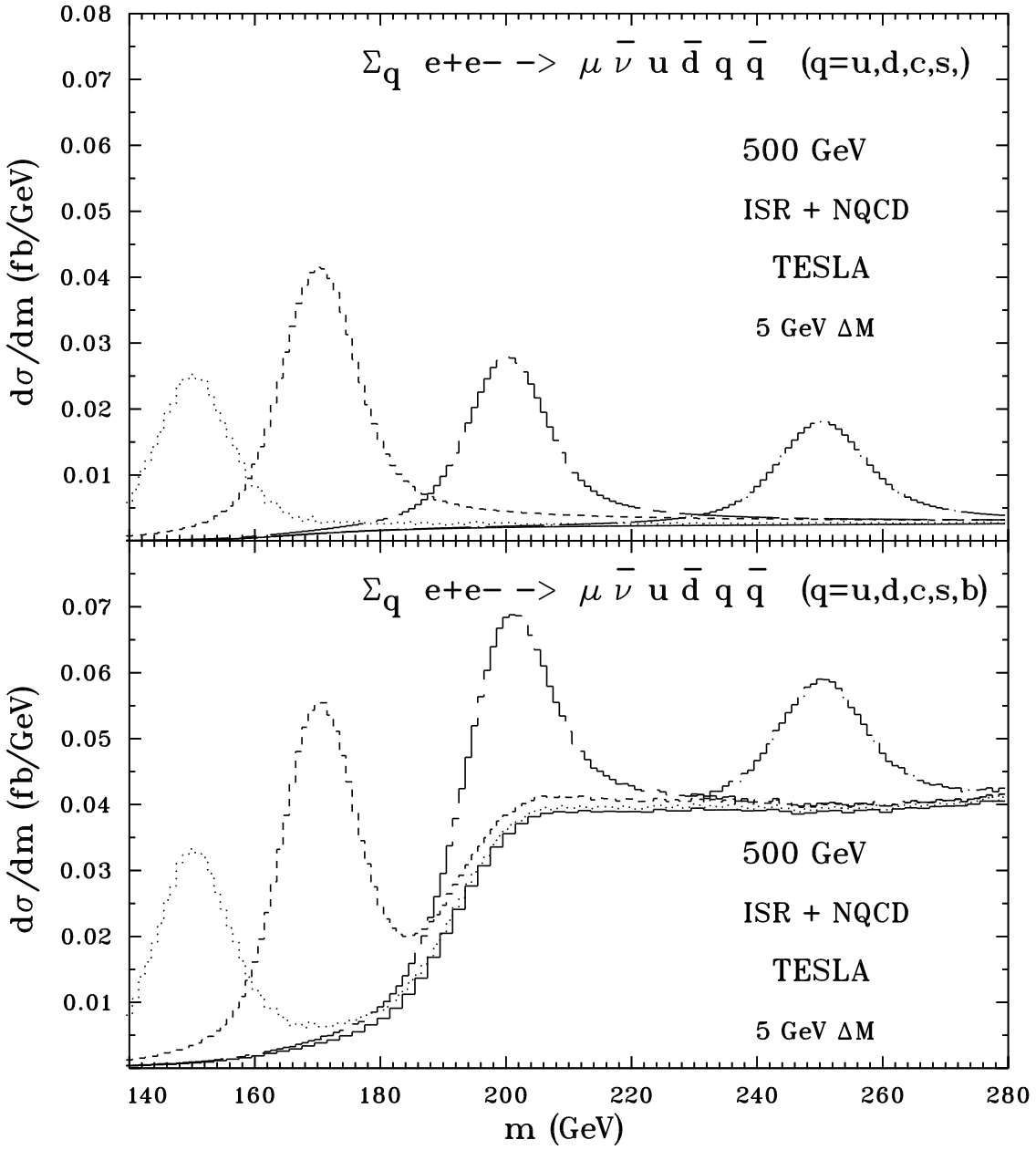

Figure 9: Reconstructed mass distributions with gaussian smearing. The continuous line represents the total background. The others correspond to the total cross sections for (from left to right) m_h= 150, 170, 200, 250 GeV. Cuts: $|m(q\bar{q}) - m_Z| < 20$ GeV, $|m(u\bar{d}) - m_W| < 20$ GeV.